© 2009 BY QUINTESSENCE PUBLISHING CO, INC. PRINTING OF THIS DOCUMENT IS RESTRICTED TO PERSONAL USE ONLY. NO PART OF THIS ARTICLE MAY BE REPRODUCED OR TRANSMITTED IN ANY FORM WITHOUT WRITTEN PERMISSION FROM THE PUBLISHER.

CT Scan–Based Finite Element Analysis of Premolar Cuspal Deflection Following Operative Procedures

*Pascal Magne, DMD, PhD**
*Tevan Oganesyan, MS***

The objective of this investigation was to present a novel method to facilitate and accelerate geometry acquisition/modification during the fabrication of finite element models of tooth restorations. Microcomputed tomographic data, stereolithography, and surface-driven automatic meshing were used to generate premolar finite element models with different occlusoproximal cavity preparations and corresponding composite resin restorations. Occlusal loading was simulated by nonlinear contact analysis. Cuspal widening was measured and correlated with existing experimental data for model validation. Cuspal widening during application of a 150-N load ranged from 2.7 μm for the unrestored tooth to 5 to 179 μm for the different preparations and 3.5 to 6.9 μm for the different restorations. The described method was efficient and generated detailed and valid three-dimensional finite element models. These models were used to study the effect of restorative procedures on cuspal deflection and revealed high cuspal strains associated with mesio-occlusodistal preparations and restorations compared to individual two-surface preparations. This study confirmed that, whenever possible during removal of interdental decay, an intact marginal ridge should be maintained to avoid three-surface preparations such as the mesio-occlusodistal and the high cuspal strain associated with this design. (Int J Periodontics Restorative Dent 2009;29:361–369.)

*Associate Professor of Dentistry, Don and Sybil Harrington Foundation Chair of Esthetic Dentistry, School of Dentistry, University of Southern California, Los Angeles, California.
**Doctoral Dental Student, School of Dentistry, University of Southern California, Los Angeles, California.

Correspondence to: Dr Pascal Magne, University of Southern California, Oral Health Center, 3151 South Hoover St., Los Angeles, CA 90089-7792; fax: +213-821-5324; email: magne@usc.edu.

A number of previous studies[1–4] analyzing biophysical stress and strain have shown that restorative procedures can make the tooth crown more deformable, and teeth could be strengthened by increasing their resistance to crown deformation. To date, a large body of experimental data has been produced about posterior teeth cuspal deflection.[5–12] These laboratory studies require sophisticated and expensive pieces of equipment, as well as large numbers of extracted teeth. To minimize confounding variables, only specimens with similar size and shape can be used, which usually limits the number of variables that can be studied. Additional problems of this type of research using extracted teeth include infection control and storage conditions.

On the other hand, in the virtual world (eg, finite element analysis), because of the nature of the original numeric model, which can be multiplied without alteration and at no cost, an infinite number of variables can be studied. The value of modeling and numeric simulation is found in the fact that it allows a researcher to define the best experimental design and select

© 2009 BY QUINTESSENCE PUBLISHING CO, INC. PRINTING OF THIS DOCUMENT IS RESTRICTED TO PERSONAL USE ONLY. NO PART OF THIS ARTICLE MAY BE REPRODUCED OR TRANSMITTED IN ANY FORM WITHOUT WRITTEN PERMISSION FROM THE PUBLISHER.

the critical variables to evaluate in an actual laboratory experiment or clinical trial. Thus, numeric simulation represents a valuable means of saving time and money associated with laboratory and clinical research.

Because of earlier hardware and software limitations, mainly two-dimensional (2D) or coarse three-dimensional (3D) models were used, which limited the type of problems studied. Nowadays, technological advancements, such as computed tomographic (CT) scan data, allow the efficient generation of sophisticated 3D models.[13–17] Those models can address a wider range of questions than earlier models. Geometry acquisition was often the most time-consuming step for the modeler. This process was prone to simplifications and errors, which could affect the results. Meshing algorithms based on patient geometry, such as the CT scan–based finite element (FE) model,[13] have revolutionized this process. For small objects such as teeth, dental implants, and dental restorations, a microCT scanner can be used.[14] However, considerable work is required to obtain smooth transitions between the different 3D objects (enamel, dentin, restoration) and precise congruent parts (sharing the exact same geometry at their interface). When a given parameter is modified (eg, restoration size), a new and separate model, including the time-consuming geometry acquisition, must be generated.

The aim of this investigation is therefore to present a novel development to facilitate and accelerate geometry acquisition/modification during the fabrication of FE models of tooth restorations. In this method, based on stereolithography (STL) and surface-driven automatic meshing, the model is built in multiple parts (using segmentation and Boolean operations with computer-assisted design [CAD] objects) based on the geometry of the unaltered tooth. Models of different restorative conditions were generated in an attempt to validate the numeric data via comparison to existing experimental data.

Method and materials

FEA preprocessing

A 3D FE model of an extracted human maxillary premolar was generated in three steps. A raw microCT set of slices was provided by Digisens (Ferney-Voltaire) with a voxel dimension of 13.67 µm. A total of 1,582 slices was provided, but only 113 slices (1 of every 14 slices) were used for the modeling.

First, an interactive medical image control system (Mimics 11.1, Materialise) was used to identify the different hard tissues visible on the scans. The Mimics program allows extended visualization and segmentation functions based on image density threshholding (Fig 1a). Enamel and dentin 3D shells (Fig 1b) are automatically created in the form of masks by growing a threshold region on the entire stack of scans. With the Mimics STL+ module, enamel and dentin were then separately converted into STL files (STL, bilinear, and interplane interpolation algorithm). The aspect ratio and connectivity of the triangles in native STLs are improper for use in FE analysis (FEA). To automatically reduce the amount of triangles and simultaneously improve their quality while maintaining geometry, the REMESH module attached to Mimics was used. The quality of the triangles is defined as a measure of triangle height/base ratio, so that the file can be imported into the FEA software package and generate optimal data. The remesh operations were applied separately to the enamel and dentin STLs.

Second, to reestablish the perfect congruence of the interfacial mesh between enamel and dentin (this congruence having been lost during the previous remeshing process), an STL handling software (MAGICS 9.9, Materialise) was used through Boolean operations (addition, intersection, or subtraction of volumes). A congruent mesh at the dentinoenamel junction was obtained, followed by additional Boolean operations with CAD objects to simulate a cylindric fixation base (embedding the root within 2 mm of the cementoenamel junction), as well as different cavity preparations (mesioocclusal [MO], mesio-occlusodistal [MOD], and slots, ie, independent mesial and distal [SLOTS]) and corresponding restorations. The exact design and dimensions of each preparation are described in Table 1 and illustrated in Fig 2. The specific dimensions of the MO and MOD models were chosen because they reproduce existing experiments by González-López et al,[11,12] which would be used in the validation process of the FEA model (see Results section).

Third, the STL files of the segmented enamel and dentin parts were

© 2009 BY QUINTESSENCE PUBLISHING CO, INC. PRINTING OF THIS DOCUMENT IS RESTRICTED TO PERSONAL USE ONLY. NO PART OF THIS ARTICLE MAY BE REPRODUCED OR TRANSMITTED IN ANY FORM WITHOUT WRITTEN PERMISSION FROM THE PUBLISHER.

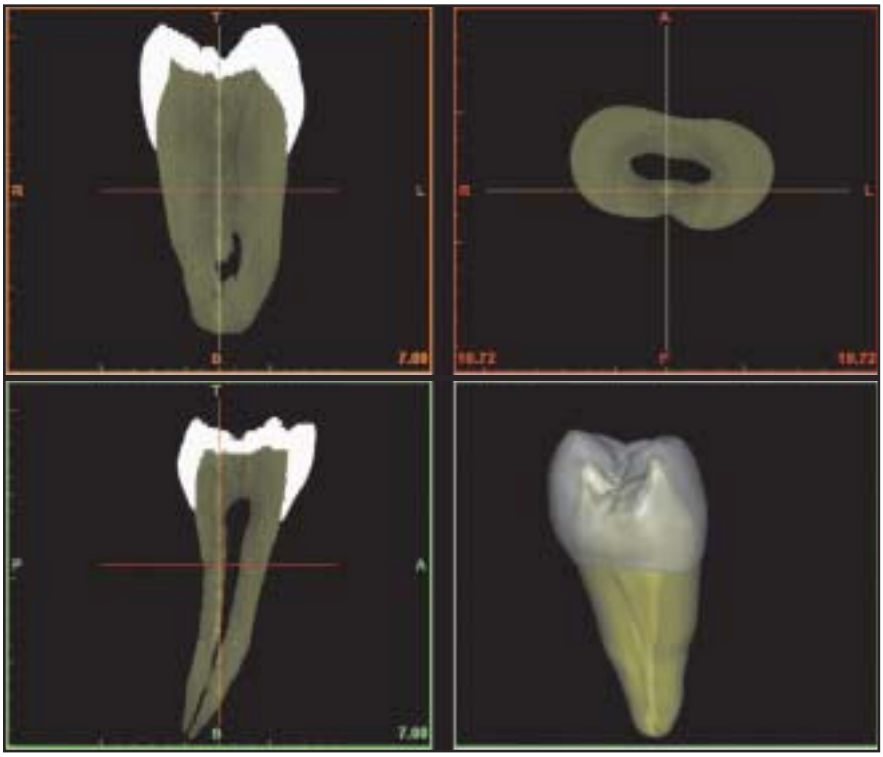

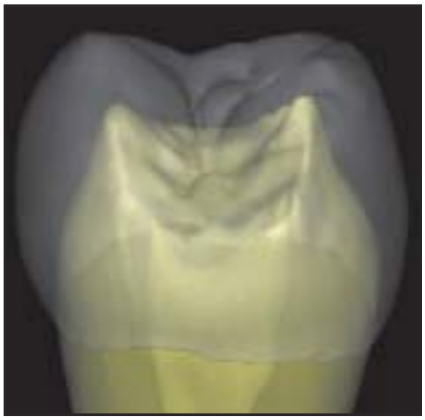

Fig 1a (left) *CT scan data as seen in Mimics 11.1. The tooth is presented in three different cross-sectional views and as a 3D object. Masks have been applied to enamel (*white*) and dentin (*yellow*) according to voxel density threshholding.*

Fig 1b (above) *Three-dimensional representation of dentin and enamel as a result of segmentation in Mimics (transparent rendering).*

Table 1 FEA geometry and characteristics for the different models

			Volumetric mesh	
Model label	**Description**	**Specific features**	**No. of elements**	**No. of nodes**
NAT	Intact natural tooth (unrestored)	Maxillary first premolar	108,534	22,080
MO_CAV	Unrestored tooth with MO preparation	Occlusal width: 3.5 mm Occlusal depth: 3.5 mm Proximal depth: 0.5 mm above CEJ	107,238	22,174
MOD_CAV	Unrestored tooth with MOD preparation	Occlusal width: 4.0 mm Proximal depth: at CEJ level	96,449	20,351
SLOTS_CAV	Unrestored tooth with independent mesial and distal slot preparations	Occlusal width: 3.5 mm Occlusal depth: 3.0 mm Proximal depth: 0.5 mm above CEJ	110,558	23,261
MO_CPR	Tooth restored with MO composite restoration	Restoration size similar to corresponding CAV model	117,879	24,061
MOD_CPR	Tooth restored with MOD composite restoration	Restoration size similar to corresponding CAV model	124,089	25,728
SLOTS_CPR	Tooth restored with independent mesial and distal composite restorations	Restoration size similar to corresponding CAV model	136,133	27,860

MO = mesioocclusal; MOD = mesio-occlusodistal; CEJ = cementoenamel junction.

© 2009 BY QUINTESSENCE PUBLISHING CO, INC. PRINTING OF THIS DOCUMENT IS RESTRICTED TO PERSONAL USE ONLY. NO PART OF THIS ARTICLE MAY BE REPRODUCED OR TRANSMITTED IN ANY FORM WITHOUT WRITTEN PERMISSION FROM THE PUBLISHER.

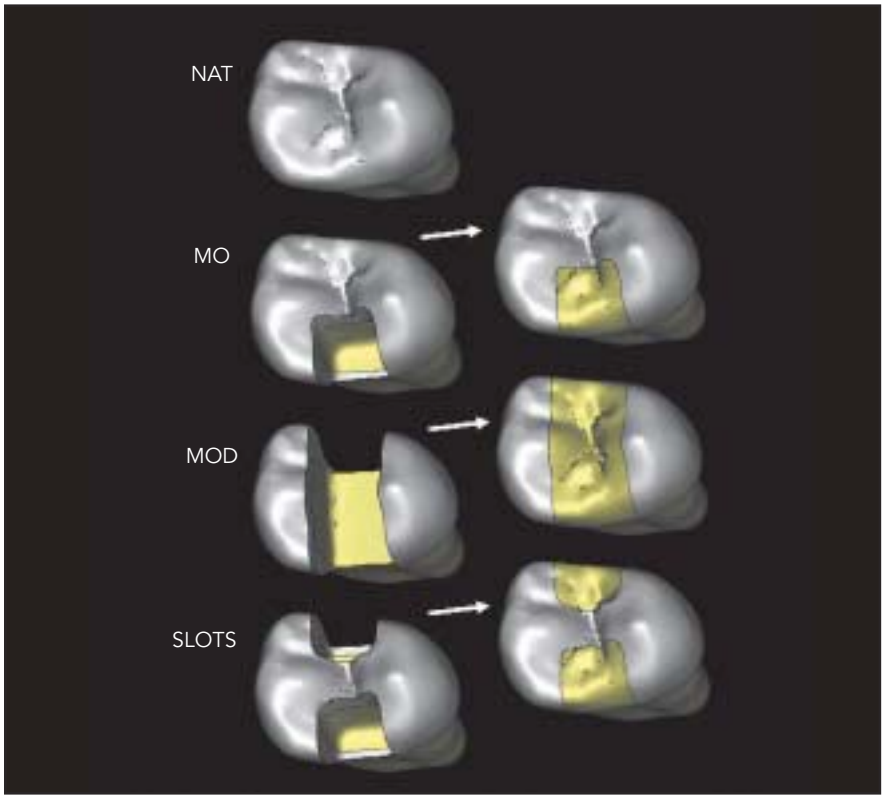

Fig 2 *Congruent STL parts of enamel and dentin resulting from Boolean intersections and subtractions between the original enamel/dentin STLs and different CAD inserts. The assembly of the different parts results in seven possible models, ie the natural tooth (NAT), MO, MOD, and SLOTS preparations as well as the corresponding composite resin restorations.*

Table 2 **Material properties**

	Elastic modulus (GPa)	Poisson ratio
Enamel	50.0	0.30[18]
Dentin	12.0	0.31[19]
Composite	10.0[20]	0.24[21]

then imported into an FEA software package (MSC.Marc/MSC.Mentat, MSC.Software). A volumetric mesh was generated automatically, and material properties were attributed (Table 2).[18–21] The triangulated STL files are optimal for automatic mesh generation using a tetrahedral mesher (tetrahedron elements with pyramidal shape and four nodal points).

Boundary conditions, loading conditions, and data processing

The nodes at the bottom surface of the stone base were assigned a fixed displacement of zero in the three spatial dimensions. The tooth and restorative materials were assumed to be bonded, simulating the use of enamel/dentin adhesives. A uniform ramp load was

© 2009 BY QUINTESSENCE PUBLISHING CO, INC. PRINTING OF THIS DOCUMENT IS RESTRICTED TO PERSONAL USE ONLY. NO PART OF THIS ARTICLE MAY BE REPRODUCED OR TRANSMITTED IN ANY FORM WITHOUT WRITTEN PERMISSION FROM THE PUBLISHER.

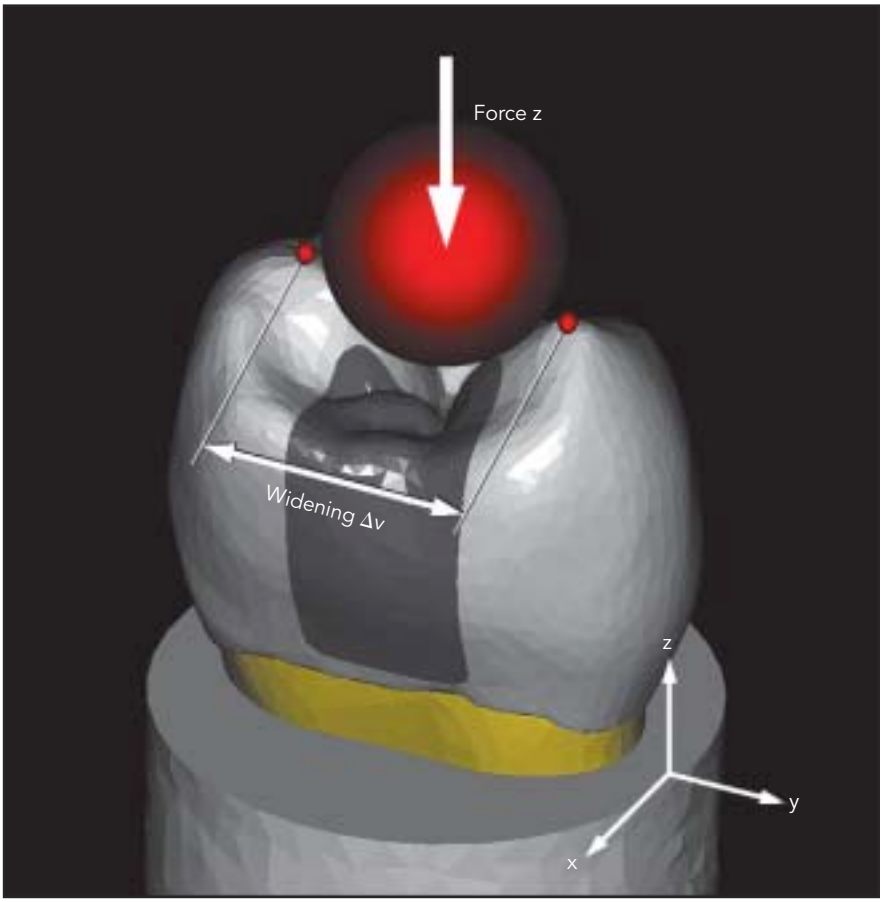

Fig 3 *Load protocol and configuration as seen in Mentat, ie, a nonlinear contact analysis between a rigid body (4.5-mm-diameter load sphere moving along the z-axis against the tooth) and a deformable tooth. The widening of the cusps (Δv) was calculated from the output values of displacement along the y-axis for selected nodes near the cusp tip.*

applied to the buccal and lingual cusps through a rigid body, ie, a 4.5-mm-diameter ball positioned as close as possible to the tooth (Fig 3). In the MOD model, the shape of the sphere had to be modified to maintain enamel occlusal contacts. The tooth was defined as a deformable contact body in a nonlinear contact analysis. Contact between the ball (defined as a rigid body) and the tooth was determined automatically by the FEA simulation during the static mechanical loading. A uniform motion was applied to the rigid ball along the z-axis through a 10-step procedure (negative velocity of 0.02 mm per step). Only one step was required to reach contact with both cusps. The motion continued for the remaining steps to reach a total force of approximately 160 N on the ball. The MSC.Marc solver was used to compute the stress and strain distributions. As mentioned earlier, these specific boundary conditions, loading protocol, and configuration were chosen because they reproduced existing experiments by González-López et al.[11,12]

© 2009 BY QUINTESSENCE PUBLISHING CO, INC. PRINTING OF THIS DOCUMENT IS RESTRICTED TO PERSONAL USE ONLY. NO PART OF THIS ARTICLE MAY BE REPRODUCED OR TRANSMITTED IN ANY FORM WITHOUT WRITTEN PERMISSION FROM THE PUBLISHER.

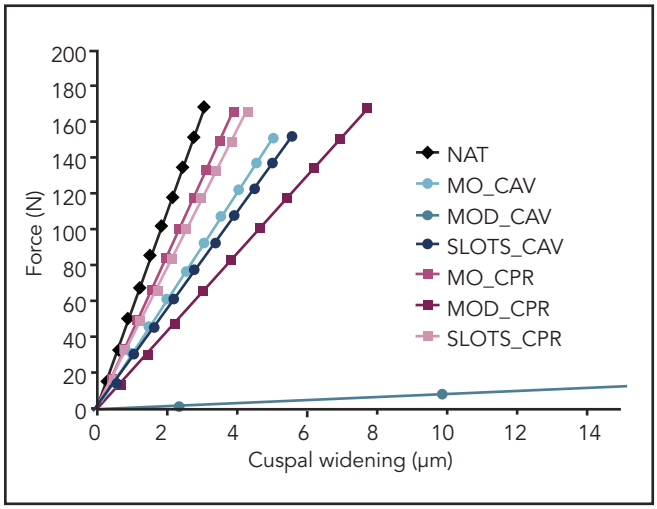

Fig 4 *Force generated by the load sphere (in Newtons) versus cuspal widening (in millimeters) for each experimental design. MO = mesioocclusal; MOD = mesio-occlusodistal; SLOTS = independent mesial and distal; CAV = cavity preparation; CPR = composite resin filling.*

Table 3 FEA results and comparison with existing experimental data (SD)

	Widening (Δv [µm]) at 150-N load (force z)		
		Gonzalez-Lopez et al	
Experimental condition	**FEA**	**2006**[11]	**2007**[12]
NAT (intact tooth)	2.7	2.6 (1.4)	2.9 (1.7)–3.7 (1.2)
MO_CAV (MO cavity)	5.0	7.2 (3.6)–8.0 (2.7)	–
MOD_CAV (MOD cavity)	179.4	114.4 (53.9)*	–
SLOT_CAV (M + D cavities)	5.4	–	–
MO_CPR (MO composite filling)	3.5	–	3.3 (1.6)
MOD_CPR (MOD composite filling)	6.9	–	8.5 (5.9)
SLOTS_CPR (M + D composite fillings)	3.8	–	–

MO = mesioocclusal; MOD = mesio-occlusodistal; M = mesial; D = distal.
*With endodontic access.

Results

The MENTAT graphic interface was used to access the postprocessing file and select specific nodes on the buccal and lingual enamel near the cusp tip. The values for displacement in the y-axis were collected for each loading step (y+ denotes displacement in the lingual direction and y– in the buccal direction). The force along the z-axis on the load sphere was also collected for each step. These data were transferred to a spreadsheet for calculation of the widening (deformation) of the cusp (by summing the displacement of each cusp). A plot of the cuspal widening against the force along the z-axis on the ball is presented in Fig 4. The linear relationship between load and deformation reveals the so-called "cuspal stiffness" (slope of the plot charting force versus deformation). The loss of tooth substance (NAT to MO_CAV to SLOTS_CAV to MOD_CAV) translated into a progressive loss of cuspal stiffness, with a dramatic decrease for MOD_CAV.

FEA validation

For validation of the models, the widening of the mesial cusp at a load of 150 N for all groups was extracted; results are presented in Table 3, along

© 2009 BY QUINTESSENCE PUBLISHING CO, INC. PRINTING OF THIS DOCUMENT IS RESTRICTED TO PERSONAL USE ONLY. NO PART OF THIS ARTICLE MAY BE REPRODUCED OR TRANSMITTED IN ANY FORM WITHOUT WRITTEN PERMISSION FROM THE PUBLISHER.

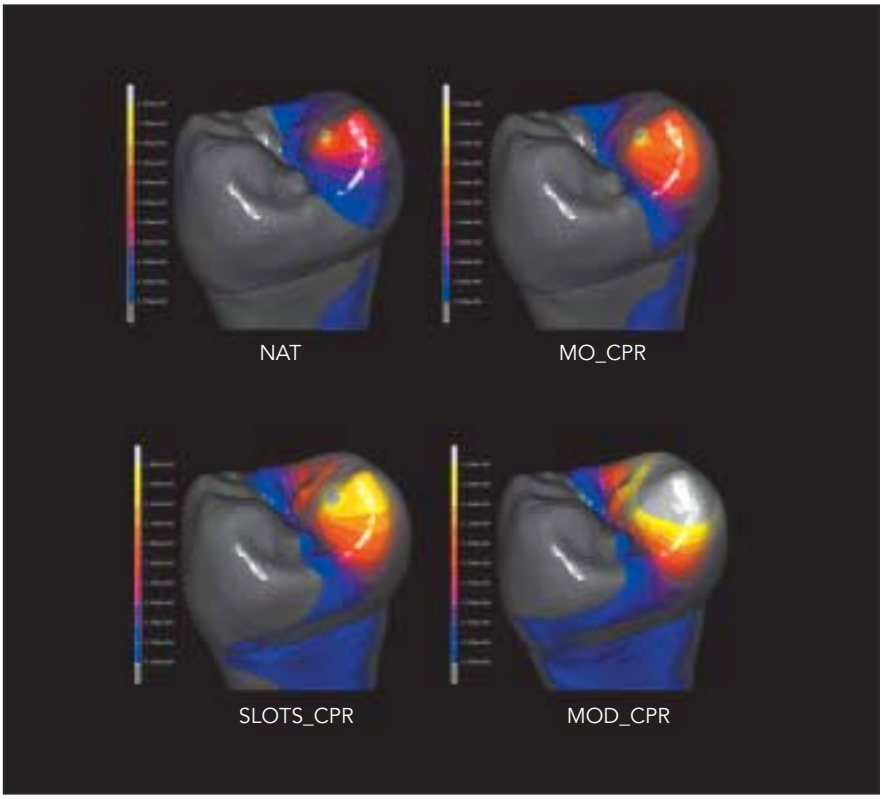

Fig 5 *Cuspal displacement (along the y-axis) in four of the seven models studied. Colors indicate positive (palatal) displacement of the palatal cusp; light gray = displacement exceeding 3 µm; dark gray = negative (buccal) displacement of the lingual cusp.*

with results from existing experiments by Gonzalez-Lopez et al,[11,12] who used the same type of tooth, loading protocol (static load at 150 N), and configuration.

There was a good association between FEA and experimental values at each restorative step, with a difference of fewer than 3 µm in most conditions. A larger difference was noted when comparing the MOD cavity in the FEA to the experimental study: 179.4 µm versus 114.4 µm, respectively. This discrepancy, however, lies close to the range of experimental data when taking into account the large standard deviations seen in the experiment.

Discussion

The standard loading protocol applied in the present analysis constitutes the most discriminating technique to study crown deformation; it also constitutes a useful validation setup that mirrors existing experimental cuspal flexure measurements. Gonzalez-Lopez et al[11,12] used a precision micrometer to measure intercuspal distance. Because the precision of this device was around 1 µm, they were not able to measure submicron displacements. Except for MOD_CAV, the maximum difference between the experimental measurements and the FEA model was around 3 µm. Considering that the corresponding standard deviations reported by both articles far exceed these values, the model can be considered valid. The results obtained with composite restored teeth are in agreement with conclusions by Douglas,[1] who stated that their strength diminishes with increasing cavity size and can only approach that of the unaltered tooth in the case of small conservative cavities, especially two-surface preparations (MO or SLOTS). Whenever possible during removal of interdental decays, an intact marginal ridge should be maintained to prevent three-surface preparations, such as the MOD and the high cuspal strain associated with this design (Fig 5). The same conclusions were drawn in the validation studies.[11,12]

© 2009 BY QUINTESSENCE PUBLISHING CO, INC. PRINTING OF THIS DOCUMENT IS RESTRICTED TO PERSONAL USE ONLY. NO PART OF THIS ARTICLE MAY BE REPRODUCED OR TRANSMITTED IN ANY FORM WITHOUT WRITTEN PERMISSION FROM THE PUBLISHER.

The approach described in the present article resulted in valid 3D models with very detailed tooth anatomy and realistic computation. Because of the previous limitations of the geometry acquisition method (eg, manual tracing of actual tooth sections) and increased computer memory requirements for 3D models, earlier attempts to generate 3D models resulted in much coarser meshes. Some authors[22,23] digitized a plaster model (crown portion) and extrapolated the inner geometry (pulp, root dentin, and enamel) using tooth morphology data from the literature. The development of a 3D FE model of a restored tooth based on a microscale CT data-acquisition technique was first described by Verdonschot et al.[14] However, the 3D geometry was obtained through the stacking of traced 2D sections, which still involved a significant amount of manual work. Moreover, the tooth was scanned after being restored with an MOD composite, such that additional scans were required to test other restorative designs.

The approach used in the present study suggests two significant improvements. First, maximum anatomic detail is obtained by surface/interface-based meshing using STL surface data. The different parts of the model, featuring different mechanical properties, are identified first (segmentation process in MIMICS) and meshed accordingly. Smooth and very well-controlled representation of interfaces such as the dentinoenamel junction is possible because elements do not overlap the different structures but strictly follow their internal boundaries. The second major development lies in the versatility of the STLs, the sophisticated visualization tools (shaded wireframe 3D views, section views, etc), and possibilities offered by the Boolean operations. The general principle of Boolean operations is that a new object can be formed by combining two 3D objects. Objects can be united, intersected, or subtracted. An essential property for the continuity of the resulting volumetric mesh is that a congruent mesh is assured at the interface between the new objects when intersecting or subtracting two overlapping objects. Unlike Verdonschot et al,[14] who had to "physically" restore the tooth before scanning it, Boolean operations with predefined CAD objects (box, cylinder, cone, or inserts) allowed the present authors to "digitally" simulate successive restorative procedures (see Fig 2), maintaining the geometry of the unaltered tooth and allowing for direct comparison with the different experimental conditions. Through the very user-friendly graphic interface of MAGICS, rapid modifications of the different parts are carried out and new STLs are generated, instantly exported, and volumetrically meshed into the FEA program.

Only 113 slices were necessary to generate these valid FEA models. With the exponential development of commercial dental CT scanners, computer processing power, and user-friendliness of interfaces, this approach should allow for rapid fabrication of patient-specific simulation of dental restorations in the very near future. Small differences may remain between reality and the FE environment. Numeric modeling, however, represents a unique way to reveal the otherwise inaccessible stress distribution within the tooth-restoration complex, and it has proven to be a useful tool in the attempt to improve the understanding of tooth biomechanics and the biomimetic approach in restorative dentistry.[24]

Conclusion

A rapid method for the generation of finite element models of dental structures and restorations has been presented. Detailed 3D FE models of a premolar tooth with different cavities and restorative designs were generated. The potential use of the model was demonstrated using nonlinear contact analysis to simulate occlusal loading. Cuspal widening was correlated with existing experimental data for model validation and optimization. The model confirmed that, whenever possible during removal of interdental decay, an intact marginal ridge should be maintained to prevent three-surface preparations such as the mesio-occlusodistal and the high cuspal strain associated with this design.

This simulation method is rapid and can readily be used for other medical applications to create patient-specific models from any other body part using either magnetic resonance imaging or computed tomography data. Further, this methodology could facilitate optimization and understanding of biomedical devices prior to animal and human clinical trials.

© 2009 BY QUINTESSENCE PUBLISHING CO, INC. PRINTING OF THIS DOCUMENT IS RESTRICTED TO PERSONAL USE ONLY. NO PART OF THIS ARTICLE MAY BE REPRODUCED OR TRANSMITTED IN ANY FORM WITHOUT WRITTEN PERMISSION FROM THE PUBLISHER.

Acknowledgments

The authors wish to express their gratitude to François Curnier (Digisens) for providing the raw microCT data. This study was supported in part by MSC.Software (MSC.Marc and MSC.Mentat) and Materialise (MIMICS and MAGICS).

References

1. Douglas WH. Methods to improve fracture resistance of teeth. In: Vanherle G, Smith DC (eds). International Symposium on Posterior Composite Resin Restorative Materials. Symposium sponsored by 3M, St. Paul, MN. The Netherlands: Peter Szulc, 1995:433–441.
2. Hood JAA. Methods to improve fracture resistance of teeth. In: Vanherle G, Smith DC (eds). International Symposium on Posterior Composite Resin Restorative Materials. Symposium sponsored by 3M, St. Paul, MN. The Netherlands: Peter Szulc, 1995:443–450.
3. Morin DL, Douglas WH, Cross M, DeLong R. Biophysical stress analysis of restored teeth: Experimental strain measurement. Dent Mater 1988;4:41–48.
4. Morin DL, Cross M, Voller VR, Douglas WH, DeLong R. Biophysical stress analysis of restored teeth: Modelling and analysis. Dent Mater 1988;4:77–84.
5. Assif D, Marshak BL, Pilo R. Cuspal flexure associated with amalgam restorations. J Prosthet Dent 1990;63:258–262.
6. Panitvisai P, Messer HH. Cuspal deflection in molars in relation to endodontic and restorative procedures. J Endod 1995; 21:57–61.
7. Pilo R, Brosh T, Chweidan H. Cusp reinforcement by bonding of amalgam restorations. J Dent 1998;26:467–472.
8. Rees JS. The role of cuspal flexure in the development of abfraction lesions: A finite element study. Eur J Oral Sci 1998;106: 1028–1032.
9. Jantarat J, Panitvisai P, Palamara JE, Messer HH. Comparison of methods for measuring cuspal deformation in teeth. J Dent 2001;29:75–82.
10. Zidan O, Abdel-Keriem U. The effect of amalgam bonding on the stiffness of teeth weakened by cavity preparation. Dent Mater 2003;19:680–685.
11. González-López S, De Haro-Gasquet F, Vílchez-Díaz MA, Ceballos L, Bravo M. Effect of restorative procedures and occlusal loading on cuspal deflection. Oper Dent 2006;31:33–38.
12. González-López S, Vílchez Díaz MA, de Haro-Gasquet F, Ceballos L, de Haro-Muñoz C. Cuspal flexure of teeth with composite restorations subjected to occlusal loading. J Adhes Dent 2007;9:11–15.
13. Cattaneo PM, Dalstra M, Frich LH. A three-dimensional finite element model from computed tomography data: A semi-automated method. Proc Inst Mech Eng [H] 2001;215:203–213.
14. Verdonschot N, Fennis WM, Kuijs RH, Stolk J, Kreulen CM, Creugers NH. Generation of 3-D finite element models of restored human teeth using micro-CT techniques. Int J Prosthodont 2001;14:310–315.
15. Cattaneo PM, Dalstra M, Melsen B. The transfer of occlusal forces through the maxillary molars: A finite element study. Am J Orthod Dentofacial Orthop 2003;123: 367–373.
16. Cattaneo PM, Dalstra M, Melsen B. The finite element method: A tool to study orthodontic tooth movement. J Dent Res 2005;84:428–433.
17. Magne P. Efficient 3D finite element analysis of dental restorative procedures using micro-CT data. Dent Mater 2007;23: 539–548.
18. Eldiwany M, Powers JM, George LA. Mechanical properties of direct and post-cured composites. Am J Dent 1993;6: 222–224.
19. Farah JW, Craig RG, Meroueh KA. Finite element analysis of three- and four-unit bridges. J Oral Rehabil 1989;16:603–611.
20. Anusavice KJ, Hojjatie B. Influence of incisal length of ceramic and loading orientation on stress distribution in ceramic crowns. J Dent Res 1988;67:1371–1375.
21. Nakayama WT, Hall DR, Grenoble DE, Katz JL. Elastic properties of dental resin restorative materials. J Dent Res 1974;53: 1121–1126.
22. Ausiello P, Apicella A, Davidson CL, Rengo S. 3D-finite element analyses of cusp movements in a human upper premolar, restored with adhesive resin-based composites. J Biomech 2001;34:1269–1277.
23. Ausiello P, Apicella A, Davidson CL. Effect of adhesive layer properties on stress distribution in composite restorations—A 3D finite element analysis. Dent Mater 2002;18:295–303.
24. Magne P, Belser U. Bonded Porcelain Restorations in the Anterior Dentition: A Biomimetic Approach. Chicago: Quintessence, 2002.

© 2009 BY QUINTESSENCE PUBLISHING CO, INC. PRINTING OF THIS DOCUMENT IS RESTRICTED TO PERSONAL USE ONLY. NO PART OF THIS ARTICLE MAY BE REPRODUCED OR TRANSMITTED IN ANY FORM WITHOUT WRITTEN PERMISSION FROM THE PUBLISHER.